Published in final edited form as:
*Virus Res*. 2009 June ; 142(1-2): 92–99. doi:10.1016/j.virusres.2009.01.014.

# Characteristics of Nipah virus and Hendra virus replication in different cell-lines and their suitability for anti-viral screening

**Mohamad Aljofan**[1,3], **Simon Saubern**[2], **Adam G. Meyer**[2], **Glenn Marsh**[1], **Joanne Meers**[3], and **Bruce A. Mungall**[1,¥]

[1] Australian Animal Health Laboratory, CSIRO Livestock Industries, Geelong, Australia

[2] CSIRO Molecular and Health Technologies, Clayton, Australia

[3] School of Veterinary Science, The University of Queensland, St. Lucia, Australia

## Abstract

We have recently described the development and validation of a High Throughput Screening assay suitable for Henipavirus antiviral identification. While we are confident this assay is robust and effective, we wished to investigate assay performance in a range of alternative cell lines to determine if assay sensitivity and specificity could be improved. We evaluated ten different cell lines for their susceptibility to Hendra and Nipah virus infection and their sensitivity of detection of the effects of the broad spectrum antiviral, ribavirin and nine novel antivirals identified using our initial screening approach. Cell lines were grouped into three categories with respect to viral replication. Virus replicated best in Vero and BSR cells, followed by Hep2, HeLa, BHK-21 and M17 cells. The lowest levels of RNA replication and viral protein expression were observed in BAEC, MMEC, A549 and ECV304 cells. Eight cell lines appeared to be similarly effective at discriminating the antiviral effects of ribavirin (<2.7 fold difference). The two cells lines most sensitive to the effect of ribavirin (ECV304 and BAEC) also displayed the lowest levels of viral replication while Vero cells were the least sensitive suggesting excess viral replication may limit drug efficacy and cell lines which limit viral replication may result in enhanced antiviral efficacy. However, there was no consistent trend observed with the other nine antivirals tested. While improvements in antiviral sensitivity in other cell lines may indicate an important role in future HTS assays, the slightly lower sensitivity to antiviral detection in Vero cells has inherent advantages in reducing the number of partially effective lead molecules identified during initial screens. Comparison of a panel of 54 novel antiviral compounds identified during routine screening of an in-house compound library in Vero, BHK-21 and BSR cells suggests no clear advantage of screening in either cell type.

### Keywords

Nipah virus; Hendra virus; antiviral; BSL4; HTS assays; ribavirin

¥Corresponding author: Dr. Bruce A. Mungall, Australian Animal Health Laboratory, CSIRO Livestock Industries, Private Bag 24, Geelong, 3220, Australia. Telephone: 61-3-52275431 Facsimile: 61-3-52275555, Email: Bruce.Mungall@csiro.au.

## 1. Background

Hendra (HeV) and Nipah (NiV) viruses are recently emerged members of the Paramyxovirus subfamily. HeV emerged in Queensland, Australia in 1994 where it caused a sudden outbreak of an acute respiratory syndrome in thoroughbred horses in a Brisbane racing stable. The syndrome was characterised by severe respiratory signs that resulted in the death of thirteen of twenty infected horses, in addition to their trainer (Murray et al., 1995). NiV emerged in Malaysia in 1998 causing fatal encephalitis in humans (Goh et al., 2000) and neurological and respiratory syndromes in pigs (Mohd Nor et al., 2000). A total of 265 cases of encephalitis, including 105 deaths, were associated with the outbreak in Malaysia (Chua et al., 2000).

There are currently no therapeutics or vaccines available to treat or prevent NiV and HeV infections (Halpin and Mungall, 2007) although a limited non-randomised trial of ribavirin during the initial NiV outbreak in Malaysia showed ribavirin therapy was able to reduce mortality of acute NiV encephalitis (Chong et al., 2001). While this study reported no serious side effects, ribavirin has been associated with a range of side effects primarily related to haemolytic anaemia (De Franceschi et al., 2000). Importantly, these viruses are also BSL4 agents that possess several biological features that make them highly adaptable for use as bioterror agents. Firstly, unlike most notable viral agents of biodefense concern such as Smallpox or Ebola, they can be isolated from natural sources (Chua et al., 2000; Halpin et al., 2000; Reynes et al., 2005) and they can be readily grown in cell culture to high titers near $1\times10^8$ $TCID_{50}$/ml (Crameri et al., 2002). NiV is highly infectious and transmitted via the respiratory tract (Field et al., 2001; Hsu et al., 2004), it can be amplified and spread in livestock serving as a source for transmission to humans, and recently it has been shown to be transmitted directly from person to person (Gurley et al., 2007; Homaira et al., 2008; Icddr, 2004b) and via contaminated food (Luby et al., 2006).

Difficulties associated with the development of effective therapeutics for these agents are primarily related to the costs associated with performing assays under BSL4 conditions, combined with the limited number of BSL4 facilities already heavily committed to research on other pathogens. Until recently, we did not have a reliable and sensitive high throughput screening (HTS) method to rapidly screen for viral inhibitors making anti-viral assessments utilising immunofluorescence highly resource intensive. We have recently proposed a HTS assay method that allows the screening of large libraries of compounds for antiviral drug discovery in vitro (Aljofan et al., 2008). This cell based assay makes use of the fact that henipaviruses rapidly replicate and produce detectable antigen in Vero cells (Crameri et al., 2002). The well established susceptibility of Vero cells to virus infection combined with their defective interferon response (Desmyter et al., 1968) provides an efficient cell-based system with which to evaluate potential antivirals, but may actually bias anti-viral screening assays. Because Vero cells replicate virus efficiently, any reduction in antigen production (also seen as a decrease in syncytia number or size via immunofluorescence) would most likely be due to an effect of the test compound rather than in response to any antiviral actions of the cells. However, this unmitigated virus susceptibility may potentially mask the detection of compounds that are only effective in high concentrations. This may reduce the number of effective lead molecules identified during the HTS process. We hypothesized that using an immune competent cell line may actually improve antiviral detection due to cooperative antiviral effects within the cell itself, and thus, may better reflect the likely effect in vivo.

In order to evaluate this possibility, we have compared a number of different cell lines using the proposed assay format to determine the level of viral infection and replication, and to assess their suitability to be used in a HTS assay format. Specifically, we were interested in the ability of each cell line to detect virus inhibition by potential antivirals from background levels of virus infection.

## 2. Materials and Methods

### 2.1. Reagents

Unless otherwise specified, all reagents were purchased from Sigma Chemical Company (St. Louis, Mo, USA). Goat anti-rabbit-AlexaFluor-488 and donkey anti-goat-AlexaFluor-488 conjugates were purchased from Invitrogen (Carlsbad, Ca, USA).

### 2.2. Cell-lines

Mouse Microvessel Endothelium Cells (MMEC) and Bovine Aortic Endothelium Cells (BAEC) were a gift from Chris Triggle. African green monkey (Vero) cells (ATCC CCL 81), baby hamster kidney cells (BHK-21), Hep-2 and HeLa cells were obtained from the American Type Culture Collection. Human Alveolar Basal Epithelial Cells (A549) were a generous gift from Eva Koziolek (CSIRO Molecular and Health Technologies, Parkville, Australia). BSR cells, a clone of BHK-21 cells (Sato et al., 1977) were a gift from Ania Gubala. ECV304 cells were obtained from Invitrogen (Carlsbad, CA, USA). Early reports indicated that ECV304 cells were a spontaneously-transformed line derived from a Japanese human umbilical vein endothelial cells (HUVEC) culture (Takahashi et al., 1990). However, several distinct differences between ECV304 and HUVEC are now apparent and recent reports have indicated genetic similarity between ECV304 and T24/83, a human bladder cancer cell line (Brown et al., 2000). M17 cells, a neuronal progenitor cell were a gift from Roberto Cappai (CSIRO Molecular and Health Technologies, Parkville, Australia). All cells except BHK-21 and BSR cells were grown in Minimal Essential Medium containing Earle's salts containing 100 U Penicillin, 100 μg/ml Streptomycin and 500 μg/ml Fungizone and 10% fetal calf serum (FCS), designated EMEM-10. BHK-21 and BSR cells were grown in EMEM-10 supplemented with 5% FCS and 5% tryptose phosphate broth (TPB) in place of 10% FCS, designated EMEM/TPB).

### 2.3. HeV and NiV

HeV was isolated in Vero cells from the lung of a horse infected in the Brisbane outbreak in October 1994 and was passaged five times in Vero cells followed by triple plaque purification and a further five passages in Vero cells as previously described (Hyatt and Selleck, 1996). NiV was isolated in Vero cells from the brain of a human fatally infected in the 1998 Malaysian outbreak and was passaged three times in Vero cells then double plaque purified and passaged a further three times in Vero cells as previously described (Shiell et al., 2003). HeV and NiV stock titres were adjusted to $1\times10^6$ $TCID_{50}$/ml. For titrations, serial ten-fold dilutions of samples were made in EMEM and 25μl transferred to five wells of a 96-well microtitre plate. Vero E6 cells in EMEM containing 10% fetal calf serum were added ($2 \times 10^4$ cells/well). Plates were incubated at 37 °C for 3–5 days and wells displaying cytopathic effect were scored as infected. Virus titre was calculated using the Reed-Meunch method (Reed and Muench, 1938) and the limit of detection was 126 $TCID_{50}$/ml virus. All work with live virus was carried out under Biosafety Level 4 (BSL4) conditions.

### 2.4. Virus infection of cell lines

Cells were seeded at a density of ($2\times10^4$) into individual wells of 96-well microtitre plates and incubated at 37 °C overnight in 100 μl EMEM-10 or EMEM/TPB as appropriate. Under BSL4 conditions, medium was removed from the plates and virus inoculum diluted in EMEM-10 was added to replicate wells of cells in volumes of 100 μl. For titration experiments, half-log dilutions of virus, commencing with $1\times10^5$ $TCID_{50}$/ml, were added to at least four replicate wells for each virus. To evaluate antiviral detection sensitivity, 100 μl of half-log dilutions of Ribavirin (10 mM-100 nM) or library compounds (20 μM-63 nM) were added to cells prior to the addition of 10,000 $TCID_{50}$/ml virus (100 μl, moi = 0.25). Plates were incubated at 37 °C

for eighteen hours. The culture medium was then discarded, plates were immersed in ice-cold absolute methanol, enclosed in heat sealed plastic bags and the bag's surface was sterilized with Microchem Plus during removal from the BSL4 laboratory. Methanol-fixed plates were air dried at room temperature for a minimum of 30 minutes prior to immunolabeling.

### 2.5. Identification of putative NiV antiviral compounds

The drug-discovery collection at CSIRO Molecular and Health Technologies (CMHT) consists of a broad range of structural classes of small molecules that have been developed during targeted drug-discovery projects for human, animal, and crop diseases (including antivirals). Implementing the HTS approach previously described for direct assessment of antiviral activity against live NiV (Aljofan et al., 2008), we have subsequently performed preliminary evaluations on over 8 000 low molecular weight molecules. First pass antiviral efficacy studies (10μM compound) identified 54 compounds exhibiting greater than 90% inhibition. Subsequent studies to determine the $IC_{50}$ of each compound against NiV infection were performed using ½ log dilutions of each compound (20 μM-63 nM) in parallel with determination of the 50% cell cytotoxicity ($CC_{50}$) to select the nine compounds with the highest calculated therapeutic indexes ($CC_{50}/IC_{50}$) for use in this study. Cytotoxicity was determined using the CellTiter-Glo® cytotoxicity kit (Promega, Madison, USA) as per the manufacturer's instructions. Briefly, Vero cell monolayers were incubated with half-log dilutions in EMEM-10 (20 μM-63 nM) of 200 μl each lead antiviral (n=3) overnight at 37 °C. Media was removed and 100 μl of CellTiter-Glo® Reagent, diluted 1:5 with chemiluminescent assay buffer, was added to each well, mixed well to lyse cells, equilibrated to room temperature for 10 min, then read using a luminometer as described above. Non-linear regression analysis performed using GraphPad Prism software to determine the $CC_{50}$.

### 2.6. HTS Immunolabeling assay

Assays were performed as previously described (Aljofan et al., 2008). Briefly, plates were washed three times with 0.01M Phosphate Buffered Saline containing 0.05% Tween-20 (PBS-T). Plates then were protein blocked with 100μl of 1% skim milk in PBS-T and incubated at 37°C for 30 minutes. After protein blocking, plates were washed three times with PBS-T, followed by incubation with 100μl anti-NiV antibody (rabbit polyclonal anti-N (Juozapaitis et al., 2007) complements of Brian Shiell) diluted 1:1 000 in PBS-T containing 1% skim milk for 30 minutes at 37 °C and then washed three times with PBS-T. Plates were incubated with 1% $H_2O_2$ for 15 minutes at room temperature then washed with PBS-T a further three times. 100μl of anti-rabbit conjugated horse radish peroxidase (HRP) diluted 1:2 000 in PBS-T containing 1% skim milk, was added to each well and plates incubated at 37 °C for 30 minutes then washed a final three times with PBS-T. For detection, 100μl of Chemiluminescent Peroxidase Substrate-3 (CPS-3) diluted 1:10 in chemiluminescent assay buffer (20 mM Tris-HCl, 1 mM $MgCl_2$, pH = 9.6) was added to each well. Plates were incubated at room temperature for 15 minutes, then read using a Luminoskan Ascent luminometer (Thermo Fisher Scientific, Waltham, USA) using 100 mSec integration per well. Raw data values for each infected well (signal) are then divided by an average of the raw data values for uninfected wells (noise) to produce signal:noise ratios for all wells.

For antiviral efficacy experiments, signal:noise values for drug treated wells were converted to % inhibition (compared to untreated, infected wells), measurements were collated and non-linear regression analysis performed using GraphPad Prism software (GraphPad Software, San Diego, CA USA) to determine the $IC_{50}$.

### 2.7. Viral antigen immunofluorescence

Methanol fixed, air dried plates were washed, protein blocked and immunolabeled with anti-NiV antisera as described above. For detection, 50μl goat-anti-rabbit IgG conjugated to Alexa-

fluor 488 (Invitrogen) diluted 1:1 000 in PBS-T containing 1% skim milk) containing 1μg/ml 4′,6-diamidino-2-phenylindole (DAPI, ICN Biomedicals, Costa Mesa, USA) was added and plates were then incubated in the dark for 30 minutes at 37 °C followed by a final wash three times with PBS-T. A total volume of 100μl of PBS-T was then added to all wells to prevent the monolayer drying out. Immunofluorescence was visualized using an Olympus IX71 inverted microscope (Olympus Australia, Mt. Waverley, Australia) coupled to an Olympus DP70 high resolution color camera. All images for analysis were obtained at an original magnification of 10x while 20x images were imported into Adobe Photoshop 7.0 for merging of Alexa-fluor 488 and DAPI images. Image analysis was performed using AnalySIS® image analysis software (Soft Imaging System GmbH, Munster, Germany) as previously described (Porotto et al., 2007). As for the HTS assay, raw data values for each infected well (signal) are then divided by an average of the raw data values for uninfected wells (noise) to produce signal:noise ratios for all wells.

### 2.8. Viral RNA isolation and Taqman PCR

After overnight virus infection, viral media was removed from cells and 150μl cell lysis buffer (RLT, Qiagen, containing 0.1% β-mercaptoethanol) was added directly to wells in 96 well plates. The cell lysate was aspirated into PCR tubes and removed from the BSL4 laboratory. RNA was extracted using the Qiagen RNeasy Mini kit as per the manufacturer's instructions. RNA was eluted in a final volume of 50μl RNase free water. Samples were stored at −20°C prior to Taqman PCR analyses.

The primers and Taqman probe to detect NiV or HeV genome sequences were designed from the N gene sequence of NiV (**AF212302**) and HeV (**AF017149**), respectively, using criteria specified in the Primer Express Software (version 1.5; Applied Biosystems, Foster City, CA). The specific NiV, HeV and 18S Taqman primers, probes and reaction conditions were used as previously reported (Mungall et al., 2006; Mungall et al., 2008). 18S rRNA was used to normalize for variations in RNA extraction. All Taqman PCR oligonucleotide primer and probe sequences used in this study are available on request.

Assays were performed in triplicate using a one-step protocol consisting of an initial reverse transcription reaction followed immediately by cDNA amplification. All Taqman reagents were purchased from Applied Biosystems except the primers, which were obtained from Geneworks. RNA (2 μl) was added to 23 μl of PCR mix in each well of a MicroAmp optical reaction plate containing 12.5 μl of Taqman OneStep PCR Mastermix, 0.625 μl of 40x Multiscribe/RNase inhibitor, 5.75 μl of distilled water, 1.25 μl each of 18 μM NiV or HeV forward and reverse primers, 1.25 μl of 5 μM HeV or NiV FAM-labeled probe, 0.125μl each of 10 μM 18SrRNAF and 18SrRNAR, and 0.125μl of 40 μM 18SrRNA-VIC-labeled probe. The samples were amplified in a GeneAmp 7500 sequence detection system (Applied Biosystems) using the following program: 48 °C for 30 min, 1 cycle; 95 °C for 10 min, 1 cycle; and 95 °C for 15 s and 60 °C for 60 s, 45 cycles. Linear regression analysis was used to quantify the NiV or HeV RNA based on cDNA standards. To correct for sample variation, $C_T$ values for viral genome in samples were normalized against 18S rRNA expression, and viral genome was expressed relative to a standard cDNA dilution (3.6 pg of cDNA).

## 3. Results

### 3.1. Henipavirus infection in different cell lines

All cell lines tested supported both HeV and NiV infection as determined by viral antigen (N protein) production (Figures 1 and 2), viral RNA replication (Figure 3) and release of infectious virus (Figure 4). BSR cells supported greater HeV and NiV replication than all other cell lines (Figures 1 and 2), followed by Vero and HeLa cells. Vero cells released the most infectious

virus (Figure 4) followed by a bovine hamster kidney (BHK) clone (BSR) and cervical epithelial (HeLa) cells. Both endothelial cell lines (BAEC and MMEC), a lung cell line (A549) and a bladder (ECV304) cell line supported the lowest levels of virus infection observed by protein expression (Figures 1 and 2), RNA expression (Figure 3) and infectious virus release (Figure 4). Human respiratory epithelial (Hep-2), neuronal (M17) cells and BHK-21 cells were all intermediate in terms of replication of either virus. There were no clear differences between virus adsorption 6h after infection as determined by N protein immunoassay and N gene Taqman PCR (data not shown) suggesting receptor mediated virus entry is not markedly different for these cell types. Definitive assessment of this process will require a quantitative measure of henipavirus receptor expression, not currently available to this study.

As we have shown previously (Aljofan et al., 2008), immunofluorescence provides a reliable confirmatory approach to quantifying viral antigen using our HTS ELISA style assay. However, despite immunofluorescence displaying a linear relationship between viral antigen expression and inoculum titer for all cell lines over four logs of virus inoculum (Figure 2), quantitation of infected monolayer immunofluorescence is significantly more labour intensive than a liquid substrate ELISA assay. Importantly, the immunofluorescence trends seen with different cell types were the same as those observed using the chemiluminescent HTS format (Figures 1 and 2). In general there was a good correlation between viral protein expression, RNA expression and infectious titer of virus released for all cell lines tested (Figures 1–4). Detection of viral genome (Figure 3) followed similar patterns to the detection of viral protein (Figure 1.) suggesting for most cell lines, infection is immediately followed by viral RNA replication which results in proportional levels of protein translation and ultimately, release of proportional amounts of infectious virus. HeV genome levels peaked for most cell lines when infected with 1,000 $TCID_{50}$ of virus while NiV genome levels continued to increase suggesting a greater capacity for NiV replication, also reflected by larger syncytia associated with NiV infection (data not shown). However, Vero cells released more infectious virus than other cell types expressing similar (HeLa, Hep 2, M17, BHK-21) or greater (BSR) amounts of viral protein (Figures 1 and 4). Similarly, BSR and HeLa cells supported greater HeV RNA replication than Vero cells, while Hep 2 and M17 cells supported greater NiV RNA replication than would be expected from their infectious virus titers (Figures 3 and 4). Interestingly, A549 cells consistently expressed some of the lowest levels of viral RNA and protein (Figures 1 and 3) yet released comparable amounts of infectious virus to BHK-21 and Hep 2 cells (Figure 4).

### 3.2. Antiviral screening strategy

In order to identify a number of positive control compounds for comparison between cell types, the broad spectrum antiviral, ribavirin, the only known commercially available inhibitor of henipavirus infection (Aljofan et al., 2008; Wright et al., 2005) and a panel of nine novel, low molecular weight compounds identified in our laboratory were used in all cell lines. These nine compounds were identified using our HTS protocol in Vero cells (Aljofan et al., 2008). This initial screening strategy involved screening all compounds in triplicate at 10 μM with the majority of compounds exhibiting between 25 and 75% inhibition of NiV infection (Figure 5). Fifty-four compounds inhibiting NiV infection by greater than 90% were identified. All compounds used for these first pass assays had been dissolved in DMSO and stored frozen for up to four years. To confirm inhibitory activity and relegate those compounds exhibiting antiviral efficacy potentially as a result of compound breakdown products, 49 compounds were sourced from lyophilised stocks and redissolved in DMSO to be retested as fresh compound. On retest, 28 of the compounds exhibited greater than 90% inhibition of NiV *in vitro*. Dose-response experiments were performed on each of these 28 compounds to determine the $IC_{50}$ concentrations in Vero cells (Figure 5). All 28 compounds exhibited $IC_{50}$ values less than 2 μM. Nine of these compounds were selected for comparison in the cell types for this study.

### 3.3. Evaluation of each cell line for HTS of antivirals

Each cell line was evaluated for its ability to discriminate decreasing concentrations of antiviral in the presence of a fixed NiV inoculum (1000 $TCID_{50}$, Table 1). Eight cell lines appeared to be similarly effective at discriminating the antiviral effects of ribavirin (<2.7 fold difference in $IC_{50}$ to Vero cells). The two cell lines most sensitive to the effect of ribavirin (ECV304 and BAEC) also displayed the lowest levels of viral replication while Vero cells were the least sensitive suggesting excess viral replication may limit drug efficacy and cell lines which limit viral replication may result in enhanced antiviral efficacy. A positive correlation was observed between ribavirin $IC_{50}$ and virus titer in each cell line ($r^2$=0.5513, Figure 6), and we observed greater variation in ribavirin $IC_{50}$s determined for cell lines producing lower titers of infectious virus (Figure 6). However, this trend was not observed with any of the other nine antivirals evaluated. Side by side comparison of a panel of 54 putative NiV antiviral compounds in Vero, BHK-21 and BSR cells revealed no clear advantage of any one cell type over another (Figure 7.). Compound $IC_{50}$ values against NiV in Vero cells correlated poorly with those obtained using either BSR cells ($r^2$=0.2881) or BHK-21 cells ($r^2$=0.1431), while the correlation between the latter two cell types ($r^2$=0.4964) improved slightly, perhaps reflecting a similar phenotype as a result of their common parental lineage.

## 4. Discussion

NiV has been responsible for a considerable number of human deaths to date during the initial emergence event in Malaysia (Chua et al., 2000) and subsequent outbreaks in India and Bangladesh (Chadha et al., 2006; Icddr, 2003; Icddr, 2004a; Icddr, 2004b; Icddr, 2005). Of particular concern, NiV has continued to re-emerge causing fatal encephalitis in humans and person-to-person transmission has been documented (Butler, 2004; Enserink, 2004; Gurley et al., 2007; Homaira et al., 2008; Hsu et al., 2004). In addition, there appeared to be direct transmission of the virus from its natural host, the flying fox, to humans, and the case mortality rate was ~70%; significantly higher than any other NiV outbreak to date. While the related HeV has only caused three human fatalities to date, it's continued re-emergence in Australia also has enormous potential for more extensive outbreaks, with considerable economic consequences. This continued pattern of re-emergence, the high fatality rates associated with these viruses and the lack of available therapies provides compelling drivers for antiviral development. The present study provides a brief comparison of NiV and HeV infection in different cell lines and an assessment of their potential for use in alternate HTS methods for assessing antiviral efficacy.

Although, most of the compared cell lines included in this study are extensively used in virology research and vaccine production, they have displayed a great variability in their response to NiV and HeV infection. Findings from the present study support earlier reports that NiV infects a wide range of mammalian cells, resulting in syncytial cell formation (Chua et al., 2000; Chua et al., 1999), but the rate of growth and patterns of cytopathic effect (CPE) produced in cell culture vary with the type of mammalian cells used (Chua, 2003). In this study, BSR and Vero cells were shown to support the highest levels of NiV and HeV virus infection quantified by viral protein expression, viral RNA expression or release of infectious virus. The observation that Vero cells support high levels of replication is not surprising. Vero cells are a stable epithelial line derived from an African Green Monkey kidney (Rhim and Schell, 1967), subsequently shown to be defective in the production of interferon (Desmyter et al., 1968), a property that has resulted in the widespread use of Vero cells for virus isolation. However, the observation that BSR cells, a clone of BHK cells, expressed viral protein at greater levels than Vero cells was unexpected. BSR cells are persistently infected with wild type rubella virus strain M-33 (Sato et al., 1977) and are routinely used for virus isolation in many laboratories. In Vero cells prolific viral replication is most likely a result of the compromised interferon

antiviral response while the persistent rubella virus infection of BSR cells may contribute to a potentially weakened innate antiviral response. Alternatively, the capsid of rubella virus has been shown to modulate genome replication of replicons and viruses (Chen and Icenogle, 2004) as observed for nucleocapsid proteins from other viruses (Hatton et al., 1992; Patton et al., 1997; Portela and Digard, 2002; Tacken et al., 2000). Thus, the presence of rubella capsid protein in BSR cells may actually increase replication of NiV and HeV potentially explaining the increase in viral protein observed in the current study.

A number of recent studies have demonstrated a potent role for NiV V and W proteins in inhibiting both interferon induction and signaling (Lo and Rota, 2008; Ludlow et al., 2008; Rodriguez et al., 2004; Rodriguez et al., 2002; Shaw et al., 2005; Shaw et al., 2004; Sleeman et al., 2008). While viral suppression of the cellular interferon response may be expected to reduce differences seen during infection of interferon defective (Vero) cells and interferon competent cells, there are clearly additional factors limiting viral replication in some of the cell lines examined here. HeLa, Hep-2, M17 and BHK-21 cells produced lower virus yields reflected in both antigen production and infectious virus titers, while endothelial, bladder and an alveolar cell line resulted in the lowest levels of virus RNA and protein expression. Curiously, A549 cells released considerable amounts of infectious NiV despite low levels of viral RNA and protein expression which contrasts with a previous study showing a good correlation between the production of infectious virus and measles virus RNA production (Helin et al., 2002). These variations may be due in part to variation in the susceptibility to viral infection between cell types, largely determined by receptor usage, and in part to variations in the level of viral replication occurring once a cell has been successfully infected. Comprehensive studies of relative receptor expression and cytokine induction events following infection will be required to appropriately answer these questions but these studies were beyond the scope of the current investigation.

While productive infection by NiV and HeV in a candidate HTS cell line is essential, we further examined their sensitivity to antiviral treatment using the only known, commercially available henipavirus inhibitor, ribavirin (Aljofan et al., 2008; Wright et al., 2005) and a panel of novel, putative antiviral compounds identified during a targeted screen of over 8 000 compounds in our drug discovery collection. The majority of cell lines evaluated appear to be approximately equal in their ability to discriminate the antiviral effects of ribavirin but varied significantly for all the other antivirals. Vero cells, which replicate infectious virus to high titers and produce high viral antigen loads, were the least effective at discriminating between antiviral concentrations, however, BSR and HeLa cells, also replicating virus to high titres, displayed ribavirin $IC_{50}$ values equivalent to most other cell lines tested. Conversely, the cell lines which appeared the most sensitive to the effects of ribavirin also had the lowest levels of viral RNA and protein expression, and the lowest infectious virus titers (with the exception of A549 cells). We note also that the lower the infectious titer observed with each cell type, the more variable the calculated ribavirin $IC_{50}$ became. Logically, these results suggest that an effective cellular antiviral response may potentiate the antiviral effects of viral replication inhibitors, thereby providing more sensitive measures of drug efficacy. Conversely, if test antivirals are effective in Vero cell assays, it is likely that in immune competent cells, this effect will be increased, suggesting that HTS using Vero cells may underestimate drug efficacy. This approach may have inherent benefits in reducing the number of potential hits identified during screening of large libraries of compounds. Interestingly, the opposite effect was seen with eight of the nine novel antivirals evaluated. For these antivirals, the observed $IC_{50}$ in Vero cells was lower than that observed in other cell lines approximately 90% of the time (excluding ribavirin and compound #23, Table 1). Does this observation reflect cellular differences with respect to virus replication and the effects of viral replication inhibitors such as ribavirin? If so this suggests that our novel compound #23 may be acting via a similar mechanism, however, without well characterised inhibitors to compare these results to, we are unable to adequately address these

questions at this time. Further studies will be needed to assess the specific mechanisms of action of each of these novel antivirals. A broader comparison of 54 novel antiviral compounds in Vero, BHK-21 and BSR cells showed no clear advantage of performing assays in any one cell type over another such that relative efficacy differences between known (well characterised) and unknown (novel) antivirals will have to suffice until clinically proven antivirals for henipavirus infection become available.

## 5. Conclusions

The current study illustrates that out of the ten cell lines tested, Vero and BSR cells were shown to support the highest levels of NiV and HeV replication. Vero cells were the least sensitive cell line for assessing antiviral efficacy while the most sensitive (and most variable) lines were endothelial and bladder cell lines, which also supported the lowest levels of viral replication. Enhanced antiviral efficacy observed in fully immune competent cell lines, compared to Vero cells, confirms recent results using RNA interference in this laboratory (Mungall et al., 2008), however, this effect may only be relevant for virus replication inhibitors. While many of the virus infection differences between cell lines may be due to receptor expression differences, variations in cytokine profiles or other cellular antiviral mechanisms, the goal of this study was to evaluate each cell line with respect to its suitability for HTS applications, rather than identifying the specific mechanisms for these individual differences. Moderation of viral infection by cells naturally may enhance the observed antiviral effects of replication inhibitors, but may also result in less stringent evaluation, ultimately resulting in a larger number of effective lead compounds identified in first pass screening assays. Paradoxically, the opposite may be true for antivirals inhibiting virus infection by alternate mechanisms. Based on these results we have elected to screen for novel antivirals using Vero cells on a larger scale eliminating many of these weak positives, but we acknowledge that this may also result in a lower number of successful drug candidates.

## Acknowledgments

BM is supported by a CSIRO Julius Award and MA is supported by an CSIRO, OCE PhD scholarship. This study was supported in part by NIH award number R21AI072396 from the National Institute of Allergy And Infectious Diseases. The content is solely the responsibility of the authors and does not necessarily represent the official views of the National Institute of Allergy And Infectious Diseases or the National Institutes of Health.

## Abbreviations

**BSL4**
: biosafety level 4

**$CC_{50}$**
: concentration resulting in 50% cytotoxicity

**DAPI**
: 4′,6-diamidino-2-phenylindole

**HeV**
: Hendra virus

**HRP**
: horse radish peroxidase

**HTS**
: high throughput screening

**$IC_{50}$**

concentration resulting in 50% inhibition

**moi**

multiplicity of infection

**NiV**

Nipah virus

**PBS-T**

phosphate buffered saline containing tween

**$TCID_{50}$**

50% tissue culture infectious dose

## References


Aljofan M, Porotto M, Moscona A, Mungall BA. Development and validation of a chemiluminescent immunodetection assay amenable to high throughput screening of antiviral drugs for Nipah and Hendra virus. J Virol Methods 2008;149:12–9. [PubMed: 18313148]

Brown J, Reading SJ, Jones S, Fitchett CJ, Howl J, Martin A, Longland CL, Michelangeli F, Dubrova YE, Brown CA. Critical evaluation of ECV304 as a human endothelial cell model defined by genetic analysis and functional responses: a comparison with the human bladder cancer derived epithelial cell line T24/83. Lab Invest 2000;80:37–45. [PubMed: 10653001]

Butler D. Fatal fruit bat virus sparks epidemics in southern Asia. Nature 2004;429:7. [PubMed: 15129247]

Chadha MS, Comer JA, Lowe L, Rota PA, Rollin PE, Bellini WJ, Ksiazek TG, Mishra A. Nipah virus-associated encephalitis outbreak, Siliguri, India. Emerg Infect Dis 2006;12:235–40. [PubMed: 16494748]

Chen MH, Icenogle JP. Rubella virus capsid protein modulates viral genome replication and virus infectivity. J Virol 2004;78:4314–22. [PubMed: 15047844]

Chong HT, Kamarulzaman A, Tan CT, Goh KJ, Thayaparan T, Kunjapan SR, Chew NK, Chua KB, Lam SK. Treatment of acute Nipah encephalitis with ribavirin. Ann Neurol 2001;49:810–3. [PubMed: 11409437]

Chua KB. Nipah virus outbreak in Malaysia. J Clin Virol 2003;26:265–75. [PubMed: 12637075]

Chua KB, Bellini WJ, Rota PA, Harcourt BH, Tamin A, Lam SK, Ksiazek TG, Rollin PE, Zaki SR, Shieh W, Goldsmith CS, Gubler DJ, Roehrig JT, Eaton B, Gould AR, Olson J, Field H, Daniels P, Ling AE, Peters CJ, Anderson LJ, Mahy BW. Nipah virus: a recently emergent deadly paramyxovirus. Science 2000;288:1432–5. [PubMed: 10827955]

Chua KB, Goh KJ, Wong KT, Kamarulzaman A, Tan PS, Ksiazek TG, Zaki SR, Paul G, Lam SK, Tan CT. Fatal encephalitis due to Nipah virus among pig-farmers in Malaysia. Lancet 1999;354:1257–9. [PubMed: 10520635]

Crameri G, Wang LF, Morrissy C, White J, Eaton BT. A rapid immune plaque assay for the detection of Hendra and Nipah viruses and anti-virus antibodies. J Virol Methods 2002;99:41–51. [PubMed: 11684302]

De Franceschi L, Fattovich G, Turrini F, Ayi K, Brugnara C, Manzato F, Noventa F, Stanzial AM, Solero P, Corrocher R. Hemolytic anemia induced by ribavirin therapy in patients with chronic hepatitis C virus infection: role of membrane oxidative damage. Hepatology 2000;31:997–1004. [PubMed: 10733558]

Desmyter J, Melnick JL, Rawls WE. Defectiveness of interferon production and of rubella virus interference in a line of African green monkey kidney cells (Vero). J Virol 1968;2:955–61. [PubMed: 4302013]

Enserink M. Emerging infectious diseases. Nipah virus (or a cousin) strikes again. Science 2004;303:1121. [PubMed: 14976284]

Field H, Young P, Yob JM, Mills J, Hall L, Mackenzie J. The natural history of Hendra and Nipah viruses. Microbes Infect 2001;3:307–14. [PubMed: 11334748]

Goh KJ, Tan CT, Chew NK, Tan PS, Kamarulzaman A, Sarji SA, Wong KT, Abdullah BJ, Chua KB, Lam SK. Clinical features of Nipah virus encephalitis among pig farmers in Malaysia. N Engl J Med 2000;342:1229–35. [PubMed: 10781618]

Gurley ES, Montgomery JM, Hossain MJ, Bell M, Azad AK, Islam MR, Molla MA, Carroll DS, Ksiazek TG, Rota PA, Lowe L, Comer JA, Rollin P, Czub M, Grolla A, Feldmann H, Luby SP, Woodward JL, Breiman RF. Person-to-person transmission of Nipah virus in a Bangladeshi community. Emerg Infect Dis 2007;13:1031–7. [PubMed: 18214175]

Halpin K, Mungall BA. Recent progress in henipavirus research. Comp Immunol Microbiol Infect Dis 2007;30:287–307. [PubMed: 17629946]

Halpin K, Young PL, Field HE, Mackenzie JS. Isolation of Hendra virus from pteropid bats: a natural reservoir of Hendra virus. J Gen Virol 2000;81:1927–32. [PubMed: 10900029]

Hatton T, Zhou S, Standring DN. RNA- and DNA-binding activities in hepatitis B virus capsid protein: a model for their roles in viral replication. J Virol 1992;66:5232–41. [PubMed: 1501273]

Helin E, Matikainen S, Julkunen I, Heino J, Hyypia T, Vainionpaa R. Measles virus enhances the expression of cellular immediate-early genes and DNA-binding of transcription factor AP-1 in lung epithelial A549 cells. Arch Virol 2002;147:1721–32. [PubMed: 12209312]

Homaira N, Rahman M, Hossain MJ, Khatun S, Nahar N, Podder G, Gurley ES, Ksiazek TG, Luby SP. Evidence of Person-to-Person Transmission of Nipah Virus Through Casual Contact. International Journal of Infectious Diseases 2008;12:e99–e99. [PubMed: 18799339]

Hsu VP, Hossain MJ, Parashar UD, Ali MM, Ksiazek TG, Kuzmin I, Niezgoda M, Rupprecht C, Bresee J, Breiman RF. Nipah virus encephalitis reemergence, Bangladesh. Emerg Infect Dis 2004;10:2082–7. [PubMed: 15663842]

Hyatt AD, Selleck PW. Ultrastructure of equine morbillivirus. Virus Res 1996;43:1–15. [PubMed: 8822630]

Icddr B. Outbreaks of Encephalitis Due to Nipah/Hendra-like Viruses, Western Bangladesh. Health and Science Bulletin 2003;1(5):1–6.

Icddr B. Nipah Encephalitis Outbreak Over Wide Area of Western Bangladesh, 2004. Health and Science Bulletin 2004a;2(1):7–11.

Icddr B. Person-to-person transmission of Nipah virus during outbreak in Faridpur District, 2004. Health and Science Bulletin 2004b;2(2):5–9.

Icddr B. Nipah Virus Outbreak from Date Palm Juice. Health and Science Bulletin 2005;3(4):1–5.

Juozapaitis M, Serva A, Zvirbliene A, Slibinskas R, Staniulis J, Sasnauskas K, Shiell BJ, Wang LF, Michalski WP. Generation of henipavirus nucleocapsid proteins in yeast Saccharomyces cerevisiae. Virus Res 2007;124:95–102. [PubMed: 17123657]

Lo MK, Rota PA. The emergence of Nipah virus, a highly pathogenic paramyxovirus. J Clin Virol 2008;43:396–400. [PubMed: 18835214]

Luby SP, Rahman M, Hossain MJ, Blum LS, Husain MM, Gurley E, Khan R, Ahmed BN, Rahman S, Nahar N, Kenah E, Comer JA, Ksiazek TG. Foodborne transmission of Nipah virus, Bangladesh. Emerg Infect Dis 2006;12:1888–94. [PubMed: 17326940]

Ludlow LE, Lo MK, Rodriguez JJ, Rota PA, Horvath CM. Henipavirus V protein association with Polo-like kinase reveals functional overlap with STAT1 binding and interferon evasion. J Virol 2008;82:6259–71. [PubMed: 18417573]

Mohd Nor MN, Gan CH, Ong BL. Nipah virus infection of pigs in peninsular Malaysia. Rev Sci Tech 2000;19:160–5. [PubMed: 11189713]

Mungall BA, Middleton D, Crameri G, Bingham J, Halpin K, Russell G, Green D, McEachern J, Pritchard LI, Eaton BT, Wang LF, Bossart KN, Broder CC. Feline model of acute nipah virus infection and protection with a soluble glycoprotein-based subunit vaccine. J Virol 2006;80:12293–302. [PubMed: 17005664]

Mungall BA, Schopman NCT, Lambeth LS, Doran TJ. Inhibition of Henipavirus infection by RNA interference. Antivir Res. 2008In Press

Murray K, Selleck P, Hooper P, Hyatt A, Gould A, Gleeson L, Westbury H, Hiley L, Selvey L, Rodwell B. A morbillivirus that caused fatal disease in horses and humans. Science 1995;268:94–7. [PubMed: 7701348]

Patton JT, Jones MT, Kalbach AN, He YW, Xiaobo J. Rotavirus RNA polymerase requires the core shell protein to synthesize the double-stranded RNA genome. J Virol 1997;71:9618–26. [PubMed: 9371626]

Porotto M, Carta P, Deng Y, Kellogg GE, Whitt M, Lu M, Mungall BA, Moscona A. Molecular determinants of antiviral potency of paramyxovirus entry inhibitors. J Virol 2007;81:10567–74. [PubMed: 17652384]

Portela A, Digard P. The influenza virus nucleoprotein: a multifunctional RNA-binding protein pivotal to virus replication. J Gen Virol 2002;83:723–34. [PubMed: 11907320]

Reed LJ, Muench H. Simple method for estimating fifty percent end points. Am J Hygiene 1938;27:493–497.

Reynes JM, Counor D, Ong S, Faure C, Seng V, Molia S, Walston J, Georges-Courbot MC, Deubel V, Sarthou JL. Nipah virus in Lyle's flying foxes, Cambodia. Emerg Infect Dis 2005;11:1042–7. [PubMed: 16022778]

Rhim JS, Schell K. Cytopathic and plaque assay of rubella virus in a line of African green monkey kidney cells (Vero). Proc Soc Exp Biol Med 1967;125:602–6. [PubMed: 4961492]

Rodriguez JJ, Cruz CD, Horvath CM. Identification of the nuclear export signal and STAT-binding domains of the Nipah virus V protein reveals mechanisms underlying interferon evasion. J Virol 2004;78:5358–67. [PubMed: 15113915]

Rodriguez JJ, Parisien JP, Horvath CM. Nipah virus V protein evades alpha and gamma interferons by preventing STAT1 and STAT2 activation and nuclear accumulation. J Virol 2002;76:11476–83. [PubMed: 12388709]

Sato M, Tanaka H, Yamada T, Yamamoto N. Persistent infection of BHK21/WI-2 cells with rubella virus and characterization of rubella variants. Arch Virol 1977;54:333–43. [PubMed: 562143]

Shaw ML, Cardenas WB, Zamarin D, Palese P, Basler CF. Nuclear localization of the Nipah virus W protein allows for inhibition of both virus-and toll-like receptor 3-triggered signaling pathways. J Virol 2005;79:6078–88. [PubMed: 15857993]

Shaw ML, Garcia-Sastre A, Palese P, Basler CF. Nipah virus V and W proteins have a common STAT1-binding domain yet inhibit STAT1 activation from the cytoplasmic and nuclear compartments, respectively. J Virol 2004;78:5633–41. [PubMed: 15140960]

Shiell BJ, Gardner DR, Crameri G, Eaton BT, Michalski WP. Sites of phosphorylation of P and V proteins from Hendra and Nipah viruses: newly emerged members of Paramyxoviridae. Virus Res 2003;92:55–65. [PubMed: 12606076]

Sleeman K, Bankamp B, Hummel KB, Lo MK, Bellini WJ, Rota PA. The C, V and W proteins of Nipah virus inhibit minigenome replication. J Gen Virol 2008;89:1300–8. [PubMed: 18420809]

Tacken MG, Rottier PJ, Gielkens AL, Peeters BP. Interactions in vivo between the proteins of infectious bursal disease virus: capsid protein VP3 interacts with the RNA-dependent RNA polymerase, VP1. J Gen Virol 2000;81:209–18. [PubMed: 10640560]

Takahashi K, Sawasaki Y, Hata J, Mukai K, Goto T. Spontaneous transformation and immortalization of human endothelial cells. In Vitro Cell Dev Biol 1990;26:265–74. [PubMed: 1690702]

Wright PJ, Crameri G, Eaton BT. RNA synthesis during infection by Hendra virus: an examination by quantitative real-time PCR of RNA accumulation, the effect of ribavirin and the attenuation of transcription. Arch Virol 2005;150:521–32. [PubMed: 15526144]

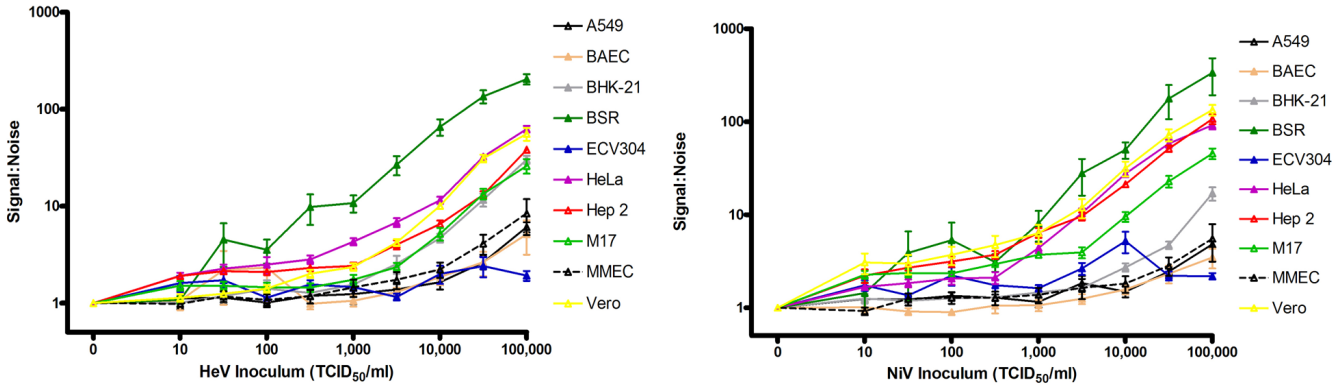


**Figure 1. Chemiluminescent immunodetection of henipavirus infection in various cell lines**

Cell lines were infected with HeV (left panel) and NiV (right panel) and viral nucleoprotein was detected in using a previously described HTS format (Aljofan et al., 2008). ½ log dilutions of virus (100μl) were incubated for 24 hours at 37 °C with 20,000 cells per well. Monolayers were fixed with methanol, air dried and immunostained with anti-NiV-N polyclonal antisera (1:1000) followed by secondary antibodies (1:2000) of Horse Radish Peroxidase conjugate with chemiluminescent (HRP-CL) detection (n=4). Values are expressed as the Mean +/− S.E.

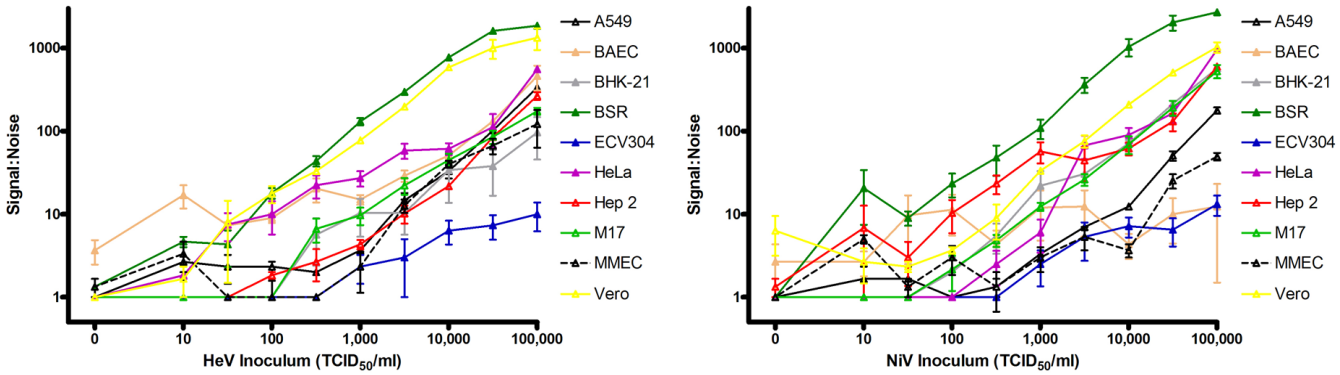


**Figure 2. Quantitation of immunofluorescent detection of henipavirus infection in cell lines**

HeV (left panel) and NiV (right panel) were inoculated onto a range of cells lines as described for Figure 1 and the number of syncytia expressing viral nucleoprotein were detected as previously described (Porotto et al., 2007) following overnight incubation. ½ log dilutions of virus (100μl) were incubated for 24 hours at 37 °C with 20,000 cells per well. Monolayers were fixed with methanol, air dried and immunostained with anti-NiV-N polyclonal antisera (1:1000) followed by detection with a fluorescent antibody Alexa-Fluor 488 conjugate (1:1000). Values are expressed as the Mean +/− S.E. (n=3).

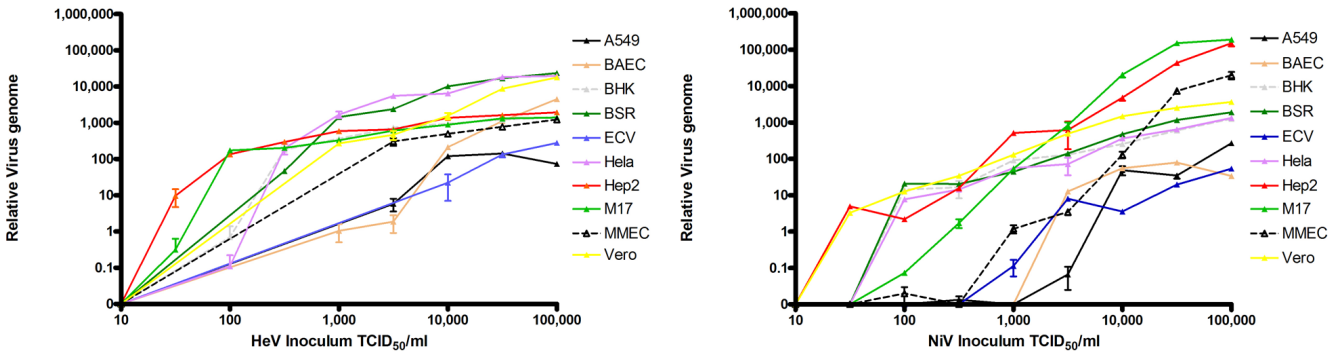


**Figure 3. Taqman PCR of henipavirus infection in various cell lines**

HeV (left panel) and NiV (right panel) were inoculated onto a range of cells lines as described for Figure 1 and viral nucleoprotein RNA detected as previously described (Mungall et al., 2006,2008). ½ log dilutions of virus (100μl) were incubated for 24 hours at 37 °C with 20,000 cells per well. Media was removed and cells were lysed with RLT buffer containing β-ME. RNA was extracted using the Qiagen RNeasy Mini kit and Taqman PCR was performed as described. Values are expressed as the Mean +/− S.E. (n=3).

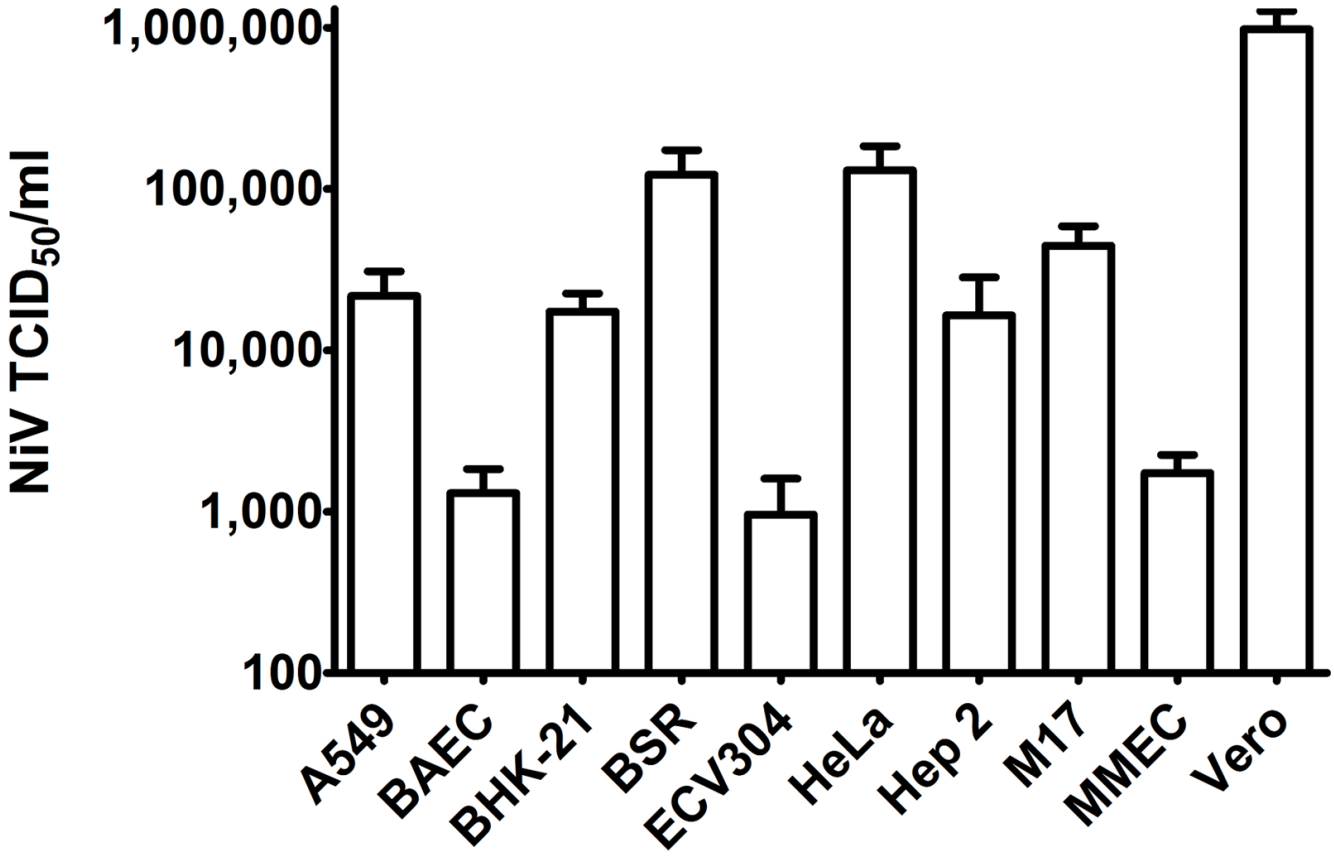


**Figure 4. Infectious titers following NiV infection in various cell lines**

Cells were infected with 10,000 $TCID_{50}$/ml NiV in 100μl for 60 min at 37 °C. Inoculum was replaced with fresh EMEM-10 and cells were incubated overnight prior to titration of cell supernatants via serial ten-fold dilutions made in EMEM-10 in 96-well microtitre plates. Vero E6 cells in EMEM-10 were added ($2 \times 10^4$ cells/well) and plates were incubated at 37 °C for 5–7 days. Wells displaying cytopathic effect were scored as infected and virus titer was calculated using the Reed-Meunch method (Reed and Muench, 1938).

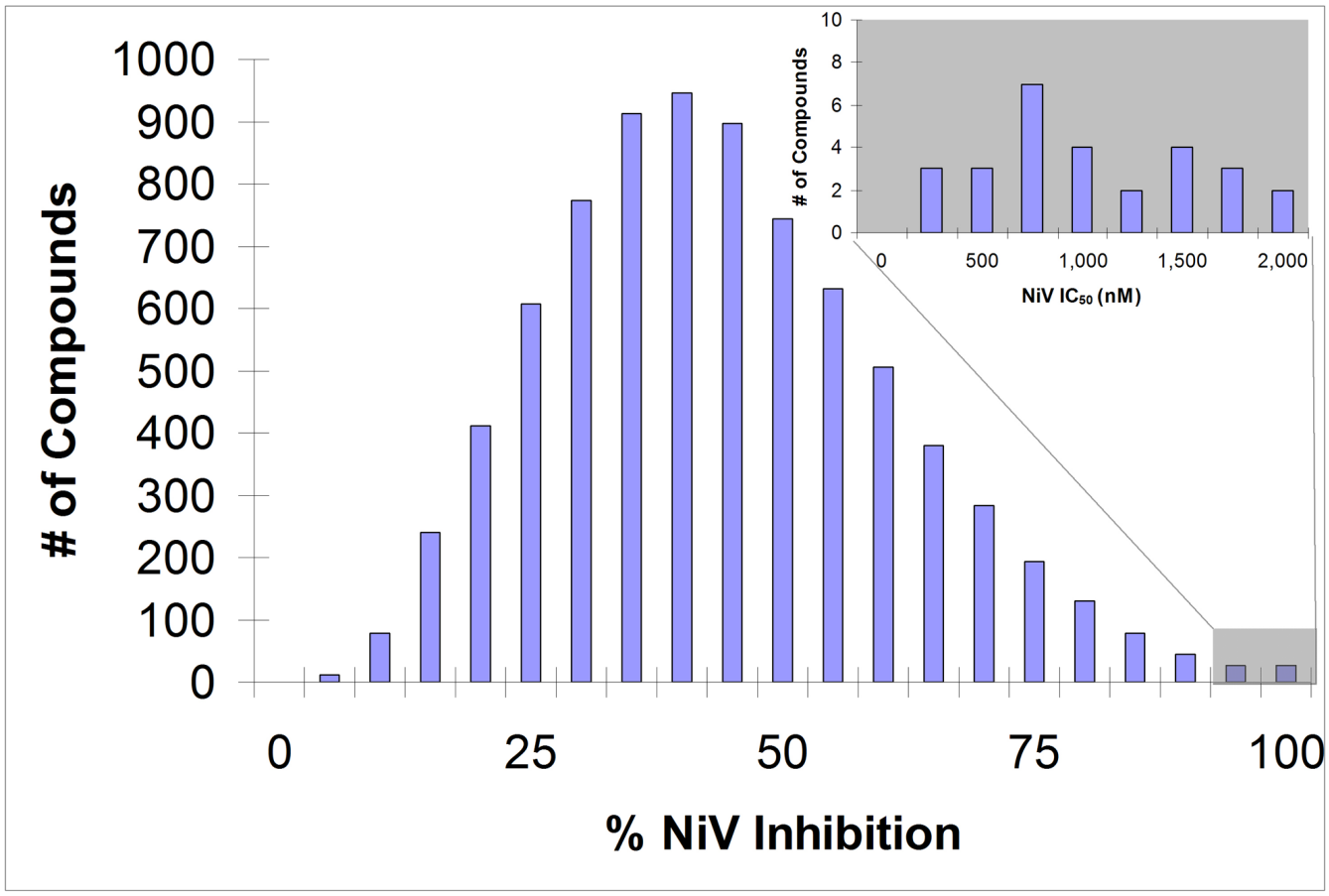


**Figure 5. HTS screening of a small compound library against live NiV**

Cells were treated with 10 μM of each compound (100μl) immediately prior to infection with 10,000 $TCID_{50}$/ml NiV in 100μl. Cells were incubated overnight at 37 °C. Monolayers were fixed with methanol, air dried and immunostained with anti-NiV-N polyclonal antisera as described above. 8,040 compounds were tested (n=3) with 54 compounds showing greater than 90% inhibition of NiV infection, while retest of freshly dissolved compound revealed 28 compounds with >90% inhibition. Dose response curves were generated for these 28 compounds (inset) showing a range of 50% inhibitory concentration ($IC_{50}$) values all less than 2 μM (n=3).

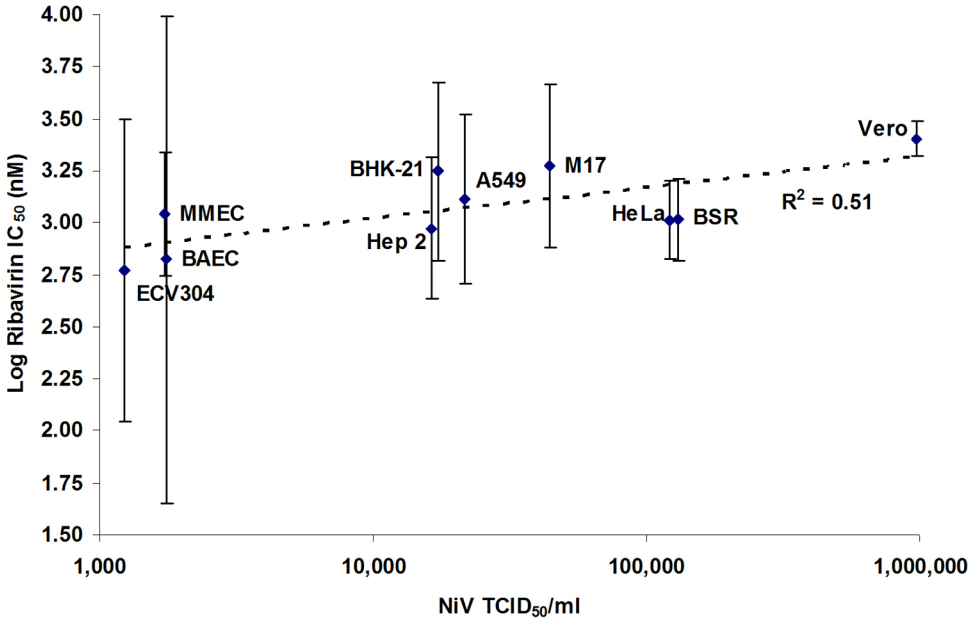


**Figure 6. Effect of ribavirin on NiV replication in various cell lines and correlation with infectious virus titer**

Cells were grown to 90% confluency in 96 well plates, log dilutions of ribavirin were added then cells infected with 10,000 $TCID_{50}$/ml NiV in 100μl. Cells were incubated overnight prior to harvesting of the cell supernatants for titration in Vero cells, or fixation of the monolayers in methanol and quantitation of viral nucleoprotein performed as described in Figure 1. Ribavirin inhibition was determined compared to untreated, infected wells and non-linear regression analysis was performed using GraphPad Prism software to determine the 50% inhibitory concentration ($IC_{50}$). Values are expressed as the Mean Log +/− S.E (n=3) ribavirin $IC_{50}$ and plotted against the infectious NiV titers recovered from untreated cell supernatants (n=3).

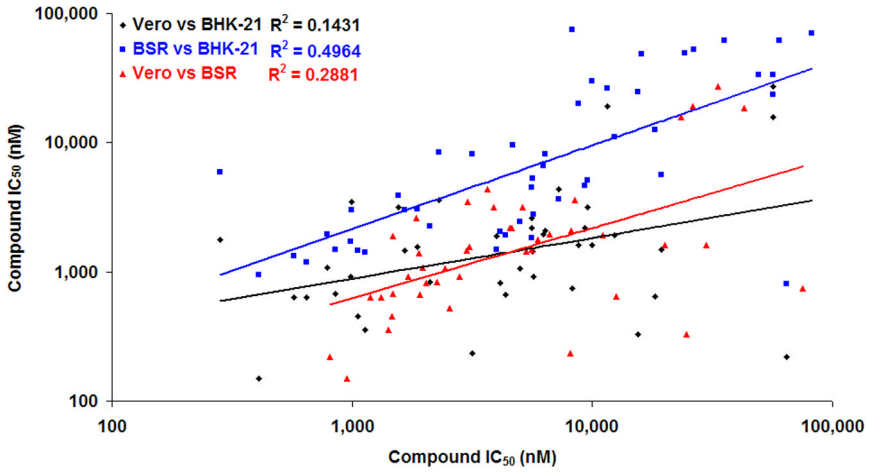


**Figure 7. Correlation between NiV antiviral efficacy in Vero, BHK-21 and BSR cells**

A panel of 54 putative NiV antiviral compounds were assayed as described for Figure 5 in Vero, BHK-21 and BSR cell lines (n=5). Non-linear regression analysis was performed using GraphPad Prism software to determine the 50% inhibitory concentration ($IC_{50}$). Average $IC_{50}$ values for each compound in each cell line are compared for each pair.

**Table 1**

Inhibition of Nipah virus by nine novel antiviral compounds and ribavirin in 10 different cell lines.

| AAHL # | A549 | BAEC | BHK21 | BSR | ECV304 | HeLa | Hep 2 | M17 | MMEC | Vero |
|---|---|---|---|---|---|---|---|---|---|---|
| **7** | 991 | 13503 | 2574 | 15631 | 22890 | 6612 | 2384 | 374 | 3305 | 2783 |
| **13** | 2792 | 1452 | 4068 | 3220 | 7300 | 14053 | 31556 | 9457 | 4647 | 1153 |
| **15** | 3384 | 195650 | 3105 | 16317 | 874 | 8223 | >1mM | DNC | >1mM | 314 |
| **16** | 2271 | 7331 | 9472 | 28556 | 1682 | 7194 | 212242 | >1mM | 3388 | 689 |
| **18** | 4180 | 3049 | >1mM | >1mM | 37753 | 1222 | >1mM | >1mM | 8644 | 1856 |
| **22** | 4697 | 4903 | 18809 | 34756 | 32794 | 5348 | 63078 | 6524 | 4172 | 558 |
| **23** | 2900 | 1832 | 111 | 203.8 | 1275 | 1136 | 2194 | 377 | 374 | 1832 |
| **33** | 475 | 782 | 1373 | 2510 | 1923 | 486 | 5480 | 4188 | 1983 | 501 |
| **42** | 342 | 2235 | 6568 | 16329 | 1653 | 14827 | 112531 | DNC | 11055 | 3093 |
| **Rib** | 1292 | 666 | 1767 | 1031 | 587 | 1036 | 941 | 1862 | 1103 | 2524 |

Values are expressed as the concentration (nM) of compound exhibiting 50% inhibition ($IC_{50}$) of NiV infection *in vitro*, determined by non-linear regression analysis after quantitative immunodetection of viral N protein expressed in ten different cell lines 24 hours post infection for six ½ log dilutions (20uM-63nM) of each compound (BHK-21 and BSR n=8, Vero n=5, all other cells n=3). Rib = ribavirin, DNC = non-linear regression curve did not converge, >1mM = $IC_{50}$ value was greater than 1 mM.